

Strain measurement in metallic glasses and metallic-glass-matrix composites by x-ray scattering

T. C. Hufnagel¹, R. T. Ott¹, and J. Almer²

¹Department of Materials Science and Engineering, Johns Hopkins University, Baltimore, Maryland USA

²Advanced Photon Source, Argonne National Laboratory, Argonne, IL 60439

Introduction

Elastic strains in both crystalline and amorphous metallic alloys can be measured *in situ* during loading, using high x-ray energy synchrotron beam lines. For instance, we have measured the elastic strain in both phases of metallic-glass-matrix composites; here, we focus on strain evolution in the amorphous matrix during uniaxial compression. We have also measured elastic strain in a single-phase metallic glass, also during uniaxial compression. Results from the composite show essentially elastic loading of the amorphous matrix up to the yield stress of the composite, in agreement with other results. Measurements on a single-phase amorphous alloy loaded in compression suggest that anelastic atomic rearrangements make a significant contribution to the macroscopic compliance of the alloy. Analysis of the radial distribution function suggests, however, that there are no significant changes in medium-range order during uniaxial compression in the elastic regime.

Methods and Materials

The specimens for this work were 3 mm diameter cylinders of either a single-phase metallic glass ($Zr_{57}Ti_5Cu_{20}Ni_8Al_{10}$) produced by arc melting and suction casting, or a metallic-glass matrix composite ($Zr_{58}Cu_{16}Ni_8Ta_8Al_{10}$) produced by a two-step melting and casting process which is described in more detail elsewhere [1]. The composite consists of relatively soft and ductile Ta-rich bcc particles (~100 μm diameter) embedded in a Zr-based amorphous matrix.

The *in situ* loading experiments were performed at beam line 1-ID of the Advanced Photon Source using 80.72 keV (0.154 \AA) x-rays with a spot size of 100 $\mu m \times 100 \mu m$. The scattering patterns were recorded on a MAR~345 image plate (150 $\mu m \times$

150 μm pixel size) placed either 400 mm (for the single-phase glass) or 975 mm (for the composite) downstream from the specimen. Intensity data were extracted by azimuthally averaging the two-dimensional ring patterns over arcs of approximately 5° centered on the vertical (loading) and horizontal (transverse) directions, using the software package FIT2D [2].

The specimen was loaded incrementally in uniaxial compression in a screw-driven load cell. The loading was paused for the x-ray exposures. To improve the signal-to-noise ratio for the single-phase glass data, 15 exposures of 10 s duration were collected and averaged to yield data for analysis. Additional details regarding the experimental procedures and data analysis can be found elsewhere [3-5].

Results and Discussion

Figure 1(a) shows the measured elastic strain (in the loading direction) in the particles of a two-phase $Zr_{58}Cu_{16}Ni_8Ta_8Al_{10}$ alloy under uniaxial compression. The particles load elastically up to a composite stress of ~350 MPa, at which point they yield. Due to the lateral constraint imposed by the matrix, with increasing composite stress (after yield) there is relatively little strain hardening. The matrix yields at ~1400 MPa composite stress, but the yielding is localized around the particles with limited shear band propagation [3]. Unloading the specimen releases causes the particles to initially unload elastically, followed by yielding in tension, resulting in a tensile residual strain in the particles when the composite stress is zero.

The matrix, in contrast (Fig. 1(b)), shows linear elasticity throughout the range of composite stresses examined. Although the particle data and finite element modeling [3] indicate that

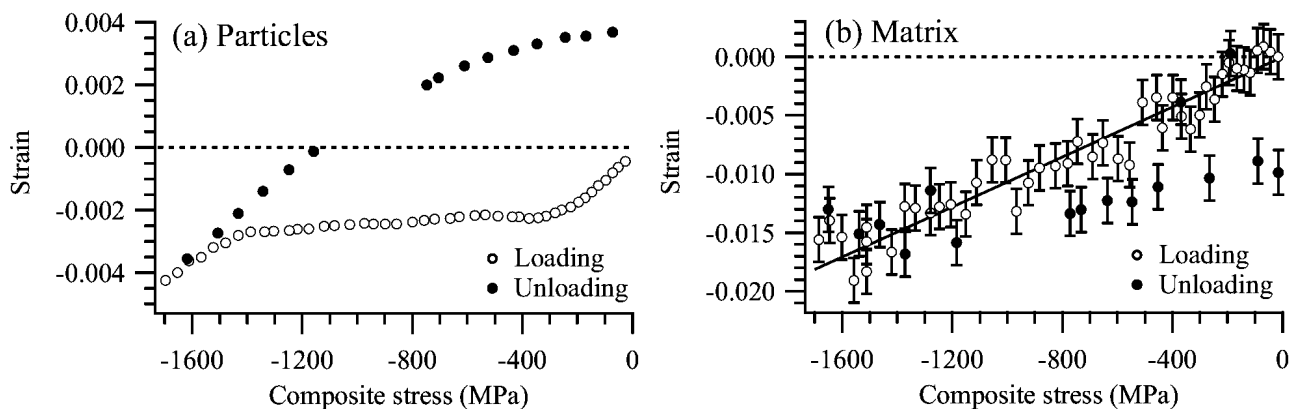


Figure 1: Elastic strain in loading direction for the (a) particles and (b) matrix in a composite specimen under uniaxial compression [5].

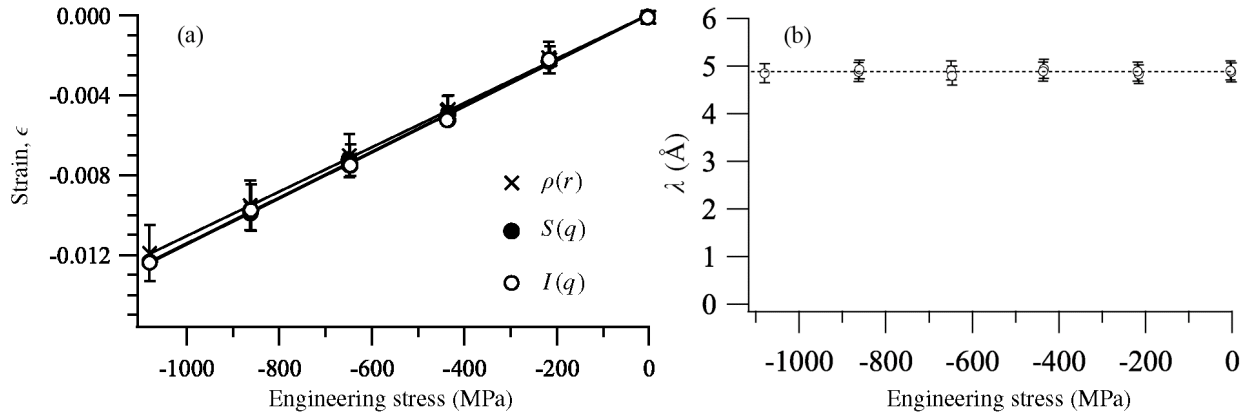


Figure 2: (a) Elastic strain in a single-phase glass under uniaxial compression. The symbols refer to the strain determined from the pair distribution function $\rho(r)$, the structure factor $S(q)$, and the raw intensity data $I(q)$ [5]. (b) The screening length λ determined from analysis of the pair correlation function, as described in the text.

the matrix yields at a composite stress of ~ 1400 MPa, no deviation from linearity is apparent (within the experimental error) in Fig. 1(b) because only a small fraction of the matrix material participates in the localized yielding around the particles. Presumably, at higher stresses (approaching the ~ 1700 MPa macroscopic yield stress) the stress-strain curve for the matrix would become nonlinear, probably displaying behavior which is nominally elastic-perfectly plastic. The discrepancy between the loading and unloading curves appears to be an experimental artifact [5].

Figure 2(a) shows the stress-strain behavior determined by x-ray scattering for a single-phase ($Zr_{57}Ti_5Cu_{20}Ni_8Al_{10}$) metallic glass. As expected, this material shows linear elastic behavior over the entire range of stresses examined (which went up to about 60% of the yield stress). However, detailed examination of the strain as a function of length scale (from the radial distribution function) shows that the strain in the first near-neighbor atomic shell is somewhat smaller than that observed for more distant pair correlations [4]. The strain at longer distances is consistent with the macroscopic Young's modulus of the amorphous alloy, while the strain for the first shell is consistent with the inherent stiffnesses of the atomic bonds estimated from the elastic properties of the crystalline elements and alloys of similar composition.

It has been proposed that a length-scale-dependent elastic modulus could result from internal atomic rearrangements on a length scale of $10\text{-}15$ Å in an amorphous alloy [6]. To examine this possibility, we apply an analysis proposed by Bodapati and coworkers [7]. We write the pair correlation function $g(r)$ as

$$g(r) = 1 + \frac{A}{r} \exp\left(\frac{-r}{\lambda}\right) \sin\left(\frac{2\pi r}{D} + \phi\right),$$

where λ is a screening length which describes the decay of short-range order, D and ϕ are constants related to the spacing of the atomic shells, and A is a scaling constant. On a plot of the peaks of $\ln[r(g(r)-1)]$ against r , the slope is $-1/\lambda$. Any significant atomic rearrangements with increasing stress would presumably show up as a change in λ . In particular, if the medium-range order increases with stress, λ should also increase. As Fig. 2(b) shows, however, λ is constant (within the experimental error) over the entire range of stresses studied. This indicates that there are no significant changes occurring in the structure beyond the first near-neighbor atomic shell of the majority of atoms in the material.

Suzuki and Egami showed, by means of computer simulations, that atomic rearrangements in a few topologically unstable regions of a metallic glass can yield anelastic effects sufficient to account for the reduced Young's modulus of the glass (compared to the corresponding crystal) [8]. Our data are consistent with this hypothesis [4]. The strain measured for the first near-neighbor is consistent with the inherent stiffnesses of the atomic bonds, but somewhat larger strains are measured over longer length scales due to the additional compliance introduced by the anelastic rearrangements. In this model no significant change in medium-range order is expected, consistent with our observation that the screening length λ is independent of stress. It is possible, however, that more significant effects would be seen at stresses closer to the yield stress of the glass. This is the subject of ongoing investigations.

Acknowledgements

Financial support for the work on the composite specimens was provided by the U.S. Department of Energy (grant FE-FG02-98ER45699) and the Army Research Laboratory (ARMAC-RTP Cooperative Agreement No. DAAD19-01-2-000315). The work on single-phase glasses was supported by the National Science Foundation (grant DMR-0307009). Use of the Advanced Photon Source was supported by the U. S. Department of Energy, Office of Science, Office of Basic Energy Sciences, under contract no. W-31-109-Eng-38.

References

- [1] C. Fan, R. T. Ott, and T. C. Hufnagel, *Appl. Phys. Lett.* 81, 1020 (2002).
- [2] A. P. Hammersley, S. O. Svensson, M. Hanland, A. N. Fitch, and D. Häusermann, *High Press. Res.* 14, 235 (1996).
- [3] R. T. Ott, F. Sansoz, J.-F. Molinari, J. Almer, K. T. Ramesh, and T. C. Hufnagel, *Acta Mater.* 53, 1883 (2005).
- [4] T. C. Hufnagel, R. T. Ott, and J. Almer, *Phys. Rev. B* 73, 064204 (2006).
- [5] T. C. Hufnagel, R. T. Ott, and J. Almer, *Mat. Res. Soc. Symp. Proc.* 903E, Z18 (2006).
- [6] H. F. Poulsen, J. A. Wert, J. Neuefeind, V. Honkimaki, and M. Daymond, *Nat. Mater.* 4, 33 (2005).
- [7] A. Bodapati, M. M. J. Treacy, M. Falk, J. Kieffer, and P. Keblinski, *J. Non-Cryst. Solids* 352, 116 (2006).
- [8] Y. Suzuki and T. Egami, *J. Non-Cryst. Solids* 75, 361 (1985).